

https://doi.org/10.1070/QEL16495

Performance investigation of optical wavelength conversion using a newly designed highly nonlinear ultra-flattened dispersion fibre

S. Selvendran, A. Sivanantharaja

Abstract. **We report an analysis of the wavelength conversion using a newly designed highly nonlinear ultra-flattened dispersion fibre (HN-UFF) for different signal modulation formats. A new technical solution is presented for high bit rate wideband wavelength conversion without any additional pump signals. Two-channel 80 Gb s^{-1} modulated signals with differential quadrature phase shift keying (DQPSK) are considered for wavelength conversion using four wave mixing (FWM) technique in a newly designed HN-UFF without additional pump signals. It is found that even when the input signal frequency spacing is increased beyond 2 THz, DQPSK modulation with carrier-suppressed return-to zero (CSRZ), or CSRZ-DQPSK, gives a better value of flattened conversion efficiency and *Q* factor. The impact of input power on conversion efficiency and effective flatness is also investigated. The performance parameters, such as conversion efficiency, *Q* factor, log of bit error rate (BER), received signal power and power penalty, are analysed.**

Keywords: *dispersion, nonlinearity, four wave mixing, wavelength conversion, modulation format.*

1. Introduction

Highly nonlinear ultra-flattened dispersion fibres (HN-UFFs) are suitable for different applications of nonlinear-optical signal processing. All optical wavelength conversion in optical fibres is a promising technology for future ultra-dense wavelength multiplexing. This largely involves the principles of optical nonlinearities such as cross-phase modulation (XPM), self-phase modulation (SPM), and four wave mixing (FWM), since they have response times only in several femto seconds [1–4]. Ultra high speed and ultra-broad band wavelength conversion [3] is possible with a tailored HN-UFF as a candidate for the wavelength router. Wavelength conversion is a technology which eliminates the traffic contention in an optical network by multicasting. It offers the flexibility to convert an optical signal from one wavelength to another using optical nonlinearities and thus eventually provides an efficient utilisation of wavelengths in the network [2, 5, 6]. Wavelength conversion in a highly nonlinear fibre (HNLF) using FWM is superior to other nonlinearities due to the transparent nature of signal bit rate and modulation format in the newly generated signals [5–7]. Until now, wavelength conversion reported was performed using FWM based on a parametric process with additional pumps [1, 2, 4, 6–14]. Zhou et al. [15] have reported two-channel 10 Gb s^{-1} wavelength conversion using FWM technique without any additional pump signal to convert a DPSK signal to a DQPSK signal format. Wu et al. [5] have also reported a novel transparent wavelength conversion for two-channel 40 Gb s^{-1} RZ–DPSK WDM signals without additional pumps. But in the proposed methods the conversion efficiency is not flattened even for the 0.6 THz input signal frequency spacing. Previously, we reported [16] uniform conversion efficiency for 50 Gb s^{-1} wavelength converted signals by reducing the HNLF length [3, 17, 18]. However a higher bit rate and higher range of flattened uniform conversion are attractive due to the constantly increasing demand for channel capacity.

In general, HNLF gives high conversion efficiency at zero dispersion wavelength (λ_{ZDW}) and the efficiency reduces drastically for wavelengths far from the λ_{ZDW} due to an increase in phase mismatch between the signals depending on the dispersion profile of the fibre [3, 19]. If HNLF has a minimal value of dispersion, a dispersion slope and a flattened dispersion curve near the zero over the wavelength spectrum, the effective bandwidth utilisation of this fibre can be increased [19]. A practical candidate, such as HN-UFF with flattened dispersion curve and good nonlinearity improves the phase matching condition between the signals which are located far from the λ_{ZDW}; therefore, the conversion efficiency can also be improved for far wavelength signals. Hence flattening of conversion efficiency can be performed over a wide wavelength spectrum. The conversion efficiency [20] of the newly generated signal achievable using FWM technique in HNLF is given by the expression

$$\eta = \frac{\alpha^2}{\alpha^2 + \Delta\beta^2}\left[1 + \frac{4\exp(-\alpha L)\sin^2(\Delta\beta L/2)}{(1-\exp(-\alpha L))^2}\right], \quad (1)$$

where L is the fibre length, and α is the loss coefficient. The expressions for propagation constant difference (phase mismatch) $\Delta\beta$ associated with wave generation at ω_3 and ω_4 are expressed as,

$$\Delta\beta(\omega_3) = 2\beta(\omega_1) - \beta(\omega_2) - \beta(\omega_3),$$

$$\Delta\beta(\omega_4) = 2\beta(\omega_2) - \beta(\omega_1) - \beta(\omega_4).$$

By reducing the $\Delta\beta$ value, as stated earlier the phase matching condition between the input signal of ω_1 and ω_2 can be improved and thus the mutual interaction (reduce the walk

S. Selvendran CVR college of Engineering, Ibrahimpatnam (M), R.R District, Telangana, India; e-mail: selvendrans@aol.com;
A. Sivanantharaja Alagappa Chettiar Government College of Engineering and Technology, Karaikudi, Tamilnadu, India

Received 13 August 2017; revision received 29 August 2018
Kvantovaya Elektronika **49** (6) 585–592 (2019)
Submitted in English

off) between the input signals can be increased in order to transfer the maximum power to the newly generated signals. The FWM conversion efficiency [21] is optimum if $\Delta\beta$ is zero, but it is quite difficult to attain. However, an optimal value can be reached with the help of HN-UFF. Such HN-UFF should necessarily have a uniformly distributed very low dispersion over the broad range of the optical spectrum and this enables to achieve a merely zero value for $\Delta\beta$. In equation (2),

$$\Delta\beta(\omega_3,\omega_4) \approx 2\pi c\frac{\Delta\lambda^2}{\lambda_m^2}\left[D(\lambda_m) \pm \frac{\Delta\lambda}{2}\frac{dD}{d\lambda}|_{\lambda_m}\right] \quad (2)$$

by reducing the dispersion D, the FWM interaction can be enhanced [20]. Here, the plus sign is used for $\Delta\beta(\omega_3)$, the minus sign is used for $\Delta\beta(\omega_4)$, and $\Delta\lambda = \lambda_1 - \lambda_2$. The adverse effect of FWM is that the conversion efficiency largely depends on input signal frequency spacing. It can be overcome to a greater extent by employing HN-UFF.

In this paper a two-channel wavelength conversion through the FWM technique in HN-UFF is proposed. The controlled dispersion flattened profile, with very good nonlinear properties of HN-UFF allows the wavelength conversion of a two-channel 80 Gb s^{-1} signal with flattened conversion efficiency over the full scope of the spectrum. CSRZ-DQPSK modulation in the transmitter section has a spectrum comprised of a carrier suppressed double side rf clock located from the center of the spectrum. This characteristic spectrum results in the improvement of overall system performance, such as receiver sensitivity, power tolerance, spectral efficiency and nonlinear impairment tolerance [22]. The performance of wavelength conversion in HN-UFF and the performance enhancement achieved by CSRZ-DQPSK in comparison to RZ-DQPSK are analysed by studying the conversion efficiency, eye diagram and Q factor.

2. Experiment setup

Figure 1 shows the experimental setup to analyse the two channel wavelength conversion without additional pump signals using HN-UFF. Here a two channel 80 Gb s^{-1} CSRZ-DQPSK wavelength-division multiplexed (WDM) signal is considered as it has a higher conversion efficiency factor when compared to RZ-DQPSK [22]. The difference between the spectra of a CSRZ-DQPSK modulated signal and a RZ-DQPSK signal is that the former's centre carrier frequency is suppressed, its bit rate/4 clock signal is placed at either side of the spectrum from the centre and it offers a narrow spectrum. As the center carrier is suppressed in the CSRZ-DQPSK, it offers a high nonlinear tolerance to the nonlinear effects such as XPM and SPM over conventional RZ-DQPSK. The clock signal in the spectrum ensures good receiver sensitivity, high chromatic dispersion tolerance, and high spectral efficiency. Moreover, CSRZ-DQPSK provides good power tolerance because of its very narrow spectrum.

In a CSRZ-DQPSK transmitter, two cw lasers (CW1 and CW2) are modulated using three Mach–Zehnder modulators (MZMs) to generate CSRZ-DQPSK signals. The first and second MZMs are driven by a combination of a $2^{31}-1$ pseudo-random bit sequence generator at 80 Gb s^{-1} and the DQPSK precoder provides the phase modulation (PM) required to obtain the a non-return-to zero (NRZ) DQPSK signal. This output is further regulated by the third MZM, at a 20 GHz rf clock with a bias voltage for pulse carving without phase shift, to generate CSRZ–DQPSK signals. Hence, the DQPSK modulation spectrum gets further narrowed down and side

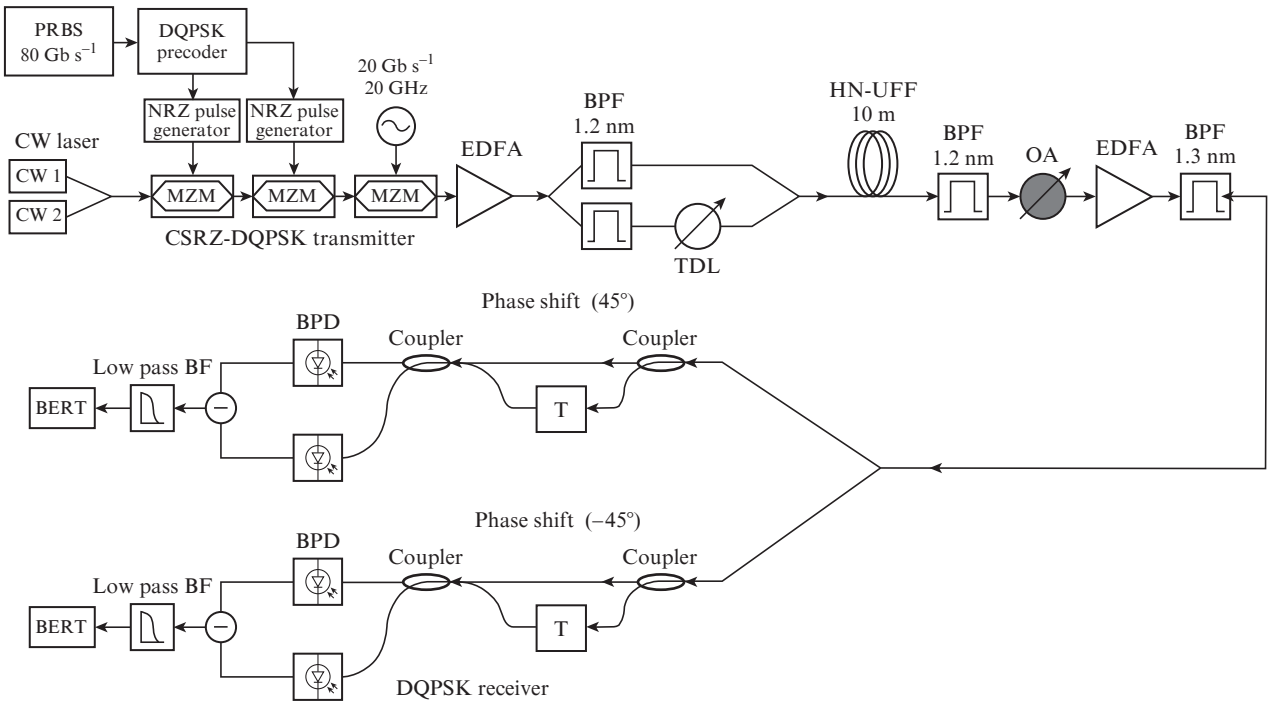

Figure 1. Experimental setup for simultaneous two channel wavelength conversion of 80 Gb s^{-1} CSRZ-DQPSK signals: (MZM) Mach–Zehnder modulator; (BPF) bandpass filter; (TDL) tunable delay line; (OA) optical attenuator; (DLI) delay-line interferometer; (BPD) balanced photodetector; (BF) Bessel filter; (T) time delay.

lobe suppression is very high. Thus, the DQPSK modulation provides higher spectral efficiency and supports a higher bit rate when compared to other modulations. The 80 Gb s^{-1} CSRZ-DQPSK signals generated are then amplified by an erbium-doped fibre amplifier (EDFA) to maintain a desired input power for HN-UFF. The EDFA must be placed before the de-correlation section so as to eliminate the amplified stimulated emission (ASE) noise produced by the EDFA because the ASE noise limits the FWM efficiency in HN-UFF.

The two input signals are separated by a sharp roll-off rectangular filter, acting as a bandpass filter. The separated signals are delayed relative to each other by a tunable time delay of 100 e^{-21} s for de-correlating the signal in order to reduce the signal overlapping and undesired interaction between the signals such as XPM. Additional rectangular filters are used in the de-correlation section to eliminate the ASE noise from the EDFA. The de-correlated signals are then sent to HN-UFF [23] with specification as shown in Table 1 for simultaneous two channel wavelength conversion. The SPM and XPM effects are minimised by decreasing the HN-UFF length to about 10 m and also by using CSRZ-DQPSK modulation. This reduced length HNLF performs ultra-fast four wave mixing (FWM) over a broad range and represents a very compact system [3]. The given CSRZ-DQPSK signals interact with this HN-UFF and produce the FWM components (wavelength converted signals) at the output.

Table 1. Parameters of HN-UFF.

Zero dispersion wavelength λ_{ZDW}/μm	1.487 and 1.9857
Dispersion slope /ps nm^{-2} km^{-1}	0.02476 at λ_{ZDW} = 1.487 μm 0.0068 at λ_{ZDW} = 1.9857 μm
Dispersion variation over S, C, L and U bands (from λ = 1.47 to 1.98 μm)/ps km^{-1} nm^{-1}	from −0.22 to 1.61 and 1.02 at λ = 1.55 μm
Nonlinear coefficient γ at λ = 1.55 μm/W^{-1} km^{-1}	9.43
PMD (1st order)/ps	0.051
Cut-off wavelength λ_c/μm	1.2759 – theory 1.2613 – ITU-T

In the receiver, the first section is a rectangular filter which acts as bandpass filter. The converted signals are filtered by a 1.2 nm filter with a sharp roll off after HN-UFF and are then sent to the pre-amplifier receiver for bit error rate (BER) measurements. The attenuator is an optional one to control the output power. In DQPSK demodulation section, in-phase and quadrature components of the filtered signal are detected by two separate sections. Each section resembles a DPSK receiver [16] but for the 2-bit time delay in asymmetric Mach–Zehnder (AMZ) interferometers and +45°, −45° phase shift in the two arms of the AMZ interferometer, so as to detect the in-phase and quadrature components of the DQPSK signal. The AMZ filter with a differential delay T converts the phase modulation into intensity modulation and allows the use of a standard direct detection (DD) receiver. Typically, in order to enhance the intrinsic receiver, a differential receiver scheme is used instead of the standard single DD receiver: two photodetectors (one for each output arm of the AMZ interferomenter) are connected to obtain the difference of the currents, which is also called the BPD configuration. After the differential receiver, a low-pass electrical Bessel filter is used for noise reduction and the output is given to bit error rate tester (BERT) terminal for measuring BER. The process of differential encoding avoids the need for a coherent detection. The EDFA is used in the receiver's pre-amplifier section to obtain good BER in converted signals. To achieve a greater power in the distribution section, another EDFA can also be included. The second rectangular filter is applied in the pass catcher to suppress the ASE noise that arises out of the EDFA and also to enhance the balanced detector output.

3. Results and discussion

Two co-propagating input 80 Gb s^{-1} CSRZ-DQPSK signals at 193 THz and 193.4 THz, denoted by A and B respectively, are considered which interact within HN-UFF. The initial frequency spacing between A and B is 0.4 THz and is increased till 2.8 THz with a step of 0.4 THz. The FWM effect is studied and various metrics such as conversion efficiency, Q factor, BER are measured. Figure 2 depicts the frequency spectrum of input signals and wavelength converted signals at initial frequency spacing of 0.4 THz, where the wavelength converted signals are denoted by A′ and B′, respectively. The conversion efficiency can be flattened to a satisfactory level by reducing the HN-UFF length [16]. Further it can also be improved by maintaining a controlled dispersion profile over the broad range of wavelength, which increases the phase matching condition between the wavelengths over the S, C, L and U bands. Figures 2 and 3 show the frequency spectrum of HN-UFF when frequency spacing between the input CSRZ-DQPSK signals is 0.4 THz and 2.4 THz, respectively. As indicated in Fig. 2, both A′ and B′ signals have equal conversion

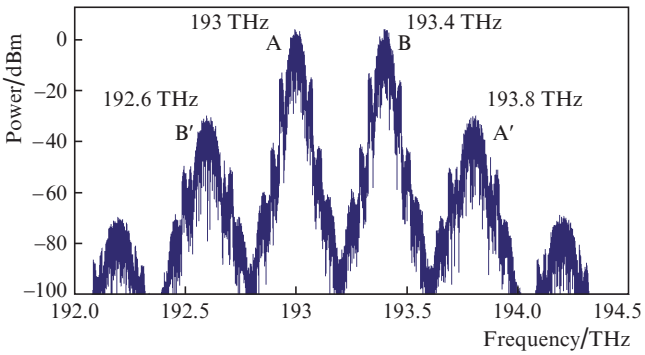

Figure 2. Frequency spectrum output of HN-UFF for input signal frequency spacing of 0.4 THz.

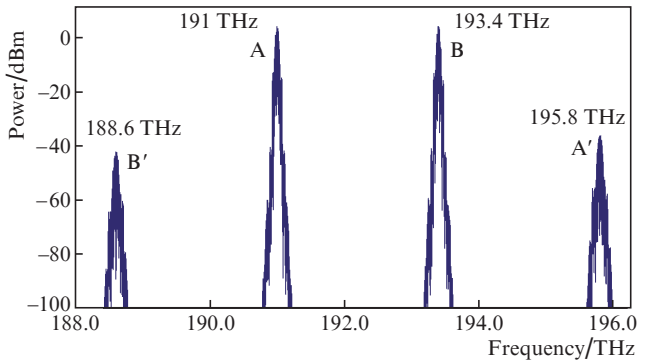

Figure 3. Frequency spectrum output of HN-UFF for input signal frequency spacing of 2.4 THz.

efficiency due to the smaller input signal frequency spacing. Usually when the frequency spacing is increased between the input signals, the conversion efficiency gets diminished as the phase matching condition is not satisfied. But in HN-UFF, this behaviour is not observed due to its flattened dispersion characteristics over a wide spectrum and a very low dispersion value, i.e. less than 1.61 ps km^{-1} nm^{-1}.

Figure 4 shows that HN-UFF allows flattened conversion efficiency of –29.9 dB with a variation of just 0.24 dB in both A′ and B′ signals up to 1.2 THz frequency spacing between the input signals. When the input signal frequency spacing is 2 THz and above, the equal conversion efficiency (uniformity) and flatness of A′ and B′ signals get disturbed due to the dispersion slope of the fibre, whose effect is greater on signal B′. As shown in Figs 3 and 4, the conversion efficiencies of B′ signals are low (below –42.15 dB) when compared to the A′ signal at an input frequency spacing of 2.4 THz. A slight variation in the dispersion slope of the fibre alters the phase matching conditions for the wavelength converted signal B′. The proposed system provides the best flattened conversion efficiency for wavelength converted signal without additional pump signals up to 1.6 THz spacing with a variation of just 0.92 dB when compared to the previously reported results [5, 15, 16].

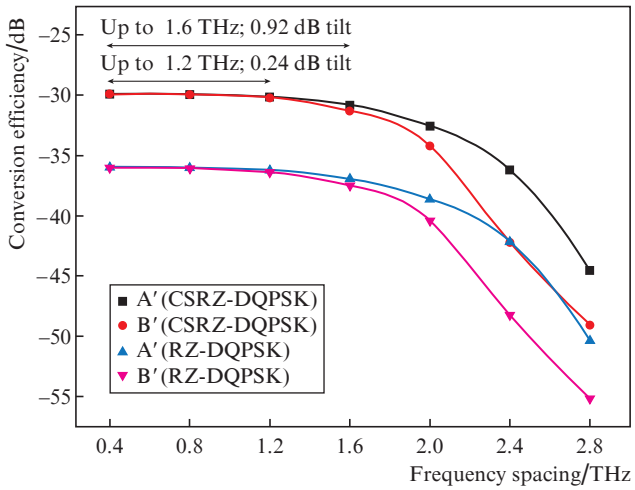

Figure 4. Conversion efficiency vs. frequency spacing for CSRZ-DQPSK and RZ-DQPSK signals.

The maximum conversion efficiency is slightly lower than that reported by Wu et al. [5], due to the reduced nonlinear coefficient of HN-UFF and the reduced fibre length of 10 m. The fibre length reduction [16] has been done intentionally to obtain flattened uniform conversion efficiency, as well as to make the system very compact. Though the 10 m HN-UFF is used, the wavelength converted signals have a very good Q factor for input signal frequency spacing up to 2 THz due to the optimal fibre parameters and power tolerance behaviour of CSRZ-DQPSK modulation. Figure 4 also compares conversion efficiencies for CSRZ-DQPSK and RZ-DQPSK modulated signals. While the CSRZ-DQPSK modulation offers conversion efficiency of –29.9 dB at the input frequency spacing of 0.4 THz, the RZ-DQPSK modulation exhibits a conversion efficiency of –35.97 dB. Even when the frequency spacing is raised to 1.6 THz, the observed variation in the conversion efficiency is very low, merely 0.92 dB.

Figure 5 shows the Q factors for CSRZ-DQPSK and RZ-DQPSK modulated signals having different input signal frequency spacings. Here also, the CSRZ-DQPSK signal demonstrates superior performance than the RZ-DPSK signal. In the case of CSRZ-DQPSK signals, both A′ and B′ have a flattened Q factor with a slight variation from 11.01 to 10.48 for input signal frequency spacing up to 2 THz. At the same time the Q factor of the RZ-DQPSK signal varies from 9.83 to 9.46 until 2 THz variation of frequency spacing at input. Beyond the 2 THz spacing equality, the Q factors of A′ and B′ get disturbed drastically for both RZ-DQPSK and CSRZ-DQPSK signals. But the CSRZ-DQPSK signal offers a very good Q factor, greater than 5.98, for both A′ and B′ signals even in the case of frequency spacing of 2.8 THz. But in the case of RZ-DQPSK, the signal gets completely disturbed and offers a very low Q factor, below the value of 3.48 under similar conditions (see Fig. 5).

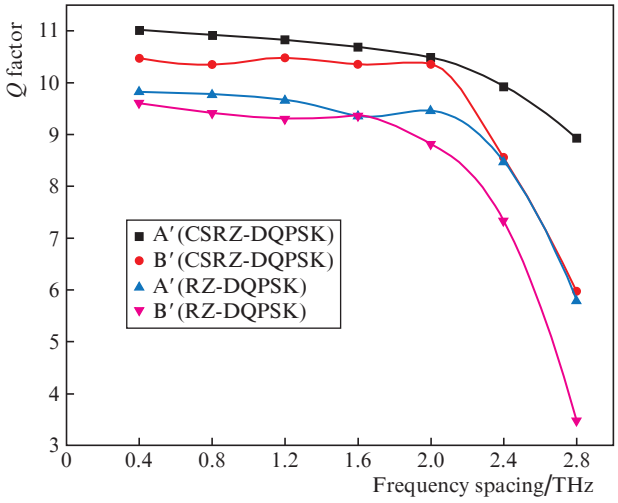

Figure 5. Quality factor vs. frequency spacing for CSRZ-DQPSK and RZ-DQPSK signals.

Figure 6 shows the eye diagrams of wavelength converted signals A′ and B′ of CSRZ-DQPSK and RZ-DQPSK modulations respectively at input signal frequency spacings of 0.8 and 2.8 THz. The eye diagrams also indicate that CSRZ-DQPSK has a better eye opening compared to the RZ-DQPSK even at the input signal frequency spacing of 2.8 THz. Further it has a higher Q factor of 8.93 and 5.98 for both A′ and B′ signals, respectively, and hence CSRZ-DQPSK is the best option for nonlinear signal processing when compared to RZ-DQPSK. From the above results, it is inferred that HN-UFF enhances the phase matching condition over a broad range of wavelengths and gives flawless flattened conversion efficiency with a better Q factor up to 1.6 THz frequency spacing between the input signals for the purpose of wavelength conversion without any additional pump signals.

Figure 7 depicts the Q factor of the given input signal after the wavelength conversion at HN-UFF output.The RZ-DQPSK modulated signal A displays a good Q factor of about 24.5 where as for the CSRZ-DQPSK signal it is 23.6. Due to the tolerant behaviour of RZ-DQPSK towards the FWM effect, it provides better quality compared to CSRZ-DQPSK. The Q factor of signal B is slightly lower than that

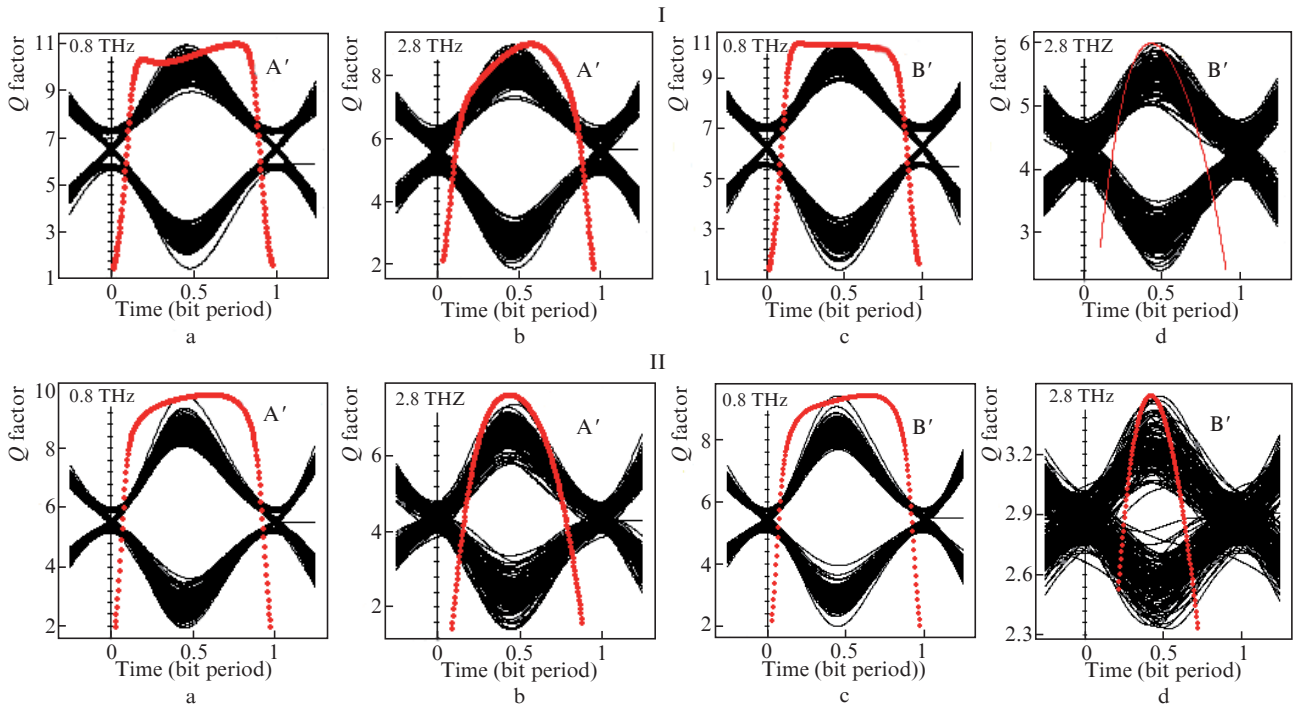

Figure 6. Eye diagrams of A′ and B′ signals of (I) CSRZ-DQPSK and (II) RZ-DQPSK at input signal frequency spacing of 0.8 and 2.8 THz: (a) A′ signal for 0.8 THz; (b) A′ signal for 2.8 THz; (c) B′ signal for 0.8 THz; and (d) B′ signal for 2.8 THz. The Q factor is shown by a dashed line.

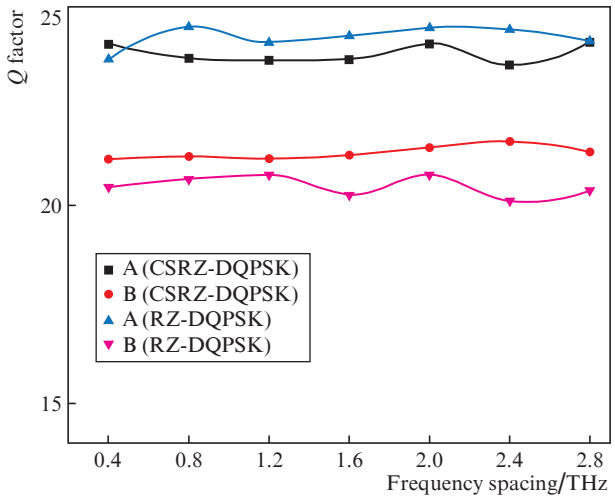

Figure 7. Quality factor of A, B signals vs.frequency spacing after HN-UFF.

of signal A. Signal B is located nearby to the ZDW with a significant power level; this permits only a small contribution from other nonlinear effect such as SPM and XPM and the Q factor is affected to a notable level compared to signal A. However the quality of the given signals is preserved and its value is about 20 even when the wavelength conversion is performed at 80 Gb s^{-1}.

The log of BER and the received signal power for the wavelength converted signals at different input signal frequency spacings are presented in Table 2. When the frequency spacing is 0.4 THz, the obtained log of BER for the CSRZ-DQPSK (A′) signal is −27.77, whereas for the RZ-DQPSK signal it is −22.37. And the received signal powers obtained are −30.32 and −38.61 dBm, respectively. When the frequency spacing is increased, the log of BER and respective received signal powers get reduced. For instance, at 2.8 THz, the log of BER and the received signal power for the RZ-DQPSK (A′) signal are −8.47 and −67.57 dBm, respectively. For the same frequency spacing the CSRZ-DQPSK signal provides −18.68 and −59.26 dBm for the log of BER and the received signal power, respectively. It follows from Table 2 that RZ-DQPSK indefensibly shows degraded performance when compared to CSRZ-DQPSK.

The power penalty is defined as what amount of input is required to recover the same BER as the normal system even after making any impairment to that system. Another way to define the power penalty is as an increase in signal power required (in dB) to maintain the same BER in the presence of impairments. Here we analyse the power penalty in wavelength converted signals with respect to frequency spacing of input signals. For this analysis, we initially maintain the BER equivalent to $1e^{-3}$ by adjusting the input power with the frequency spacing of 0.4 THz between the signals. By using the forward error correction technique (FEC), we can detect the received signal which has a BER up to $1e^{-3}$, the worst case. Beyond this level, it is difficult to detect the received signal. Hence, we have preferred this BER level as an initial value to conduct our experiment. If we increase the frequency spacing between the input signal (introduce impairment), it will affect the received BER and we can measure the power penalty for this situation. Figure 8 shows that CSRZ-DQPSK along with HN-UFF provides a very low power penalty of 0.25 dB even at the frequency spacing of 1.6 THz. This is the best ever value reported in the contemporary literature. But the RZ-DQPSK signal delivers an undesirable power penalty value of 1.72 dB and 2.49 dB for the frequency spacings of 1.6 THz and 2 THz, respectively. Due to the dispersion contribution of the fibre, the observed conversion efficiency and Q factor deviation,

Table 2. Log of BER and received signal power (A′ and B′) for the different channel frequency spacings.

Frequency spacing/THz	Log of BER				Received signal power/dBm			
	CSRZ-DQPSK		RZ-DQPSK		CSRZ-DQPSK		RZ-DQPSK	
	A′	B′	A′	B′	A′	B′	A′	B′
0.4	−27.77	−25.24	−22.37	−21.44	−30.32	−30.37	−38.61	−38.73
0.8	−27.34	−24.68	−22.14	−20.65	−30.35	−30.44	−38.66	−38.85
1.2	−26.91	−25.26	−21.69	−20.18	−30.76	−31.05	−39.09	−39.53
1.6	−26.24	−24.71	−20.42	−20.42	−32.12	−33.19	−40.51	−41.73
2	−25.29	−24.74	−20.80	−18.25	−35.41	−38.96	−43.90	−47.56
2.4	−22.81	−17.23	−16.98	−12.98	−42.71	−54.85	−51.04	−63.44
2.8	−18.68	−8.95	−8.47	−3.61	−59.26	−68.94	−67.57	−77.49

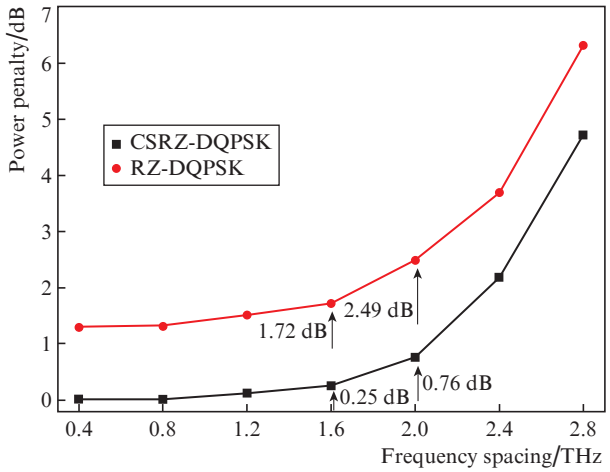

Figure 8. Power penalty vs. channel frequency spacing for the wavelength converted signals.

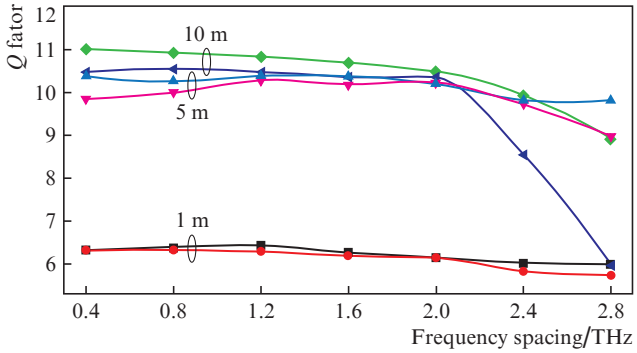

Figure 10. Quality factor of CSRZ-DQPSK signals A′ (■,▲,◆) and B′ (●,▼,◄) vs. channel frequency spacing for the fibres of length 1, 5, and 10 m.

beyond the 2 THz spacing, is eliminated by reducing the signal interaction length over the fibre. Therefore, flatness of the conversion efficiency can be improved greatly by reducing the fibre length. But the peak value of the conversion efficiency and Q factor of wavelength converted signals get diminished to a considerable level.

Figures 9 and 10 show the conversion efficiency and Q factor for the different fibre lengths. For a fibre length of 5 m the observed flattened conversion efficiency is −35.88 dB with a variation of 0.62 dB up to 2 THz channel spacing, whereas a 1 m fibre exhibits variation of −0.1 dB only even at 2.8 THz channel spacing with conversion efficiency of −49.85 dB. This reduced conversion efficiency also affects the Q factor of the wavelength converted signal. For a 1 m length of fibre, the observed Q factor for the wavelength converted signal is less than 6.4 which is equivelent to the BER value of $1e^{-10}$. This value is better than the standard BER value of $1e^{-9}$ (without FEC).

Figure 11 and 12 show the dependences of the conversion efficiency bandwidth (3 dB falling from the maximum conversion efficiency) and the Q factor of the wavelength converted

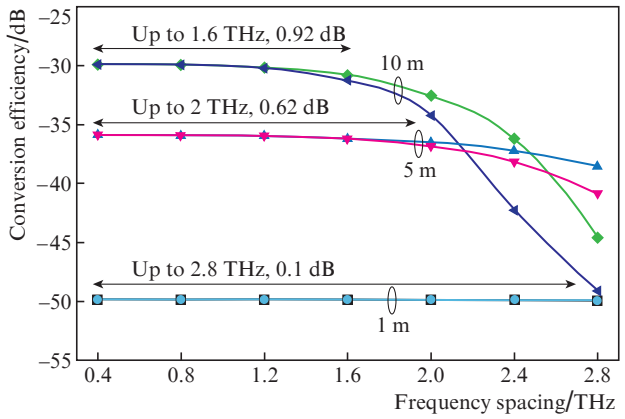

Figure 9. Conversion efficiency of CSRZ-DQPSK signals A′ (■,▲,◆) and B′ (●,▼,◄) vs. channel frequency spacing for the different fibres of length 1, 5 and 10 m.

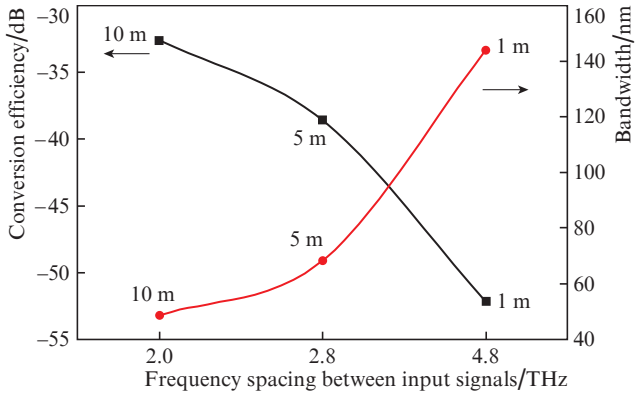

Figure 11. Conversion efficiency (■) and bandwidth (●) vs. channel frequency spacing for fibres of length 1, 5, and 10 m.

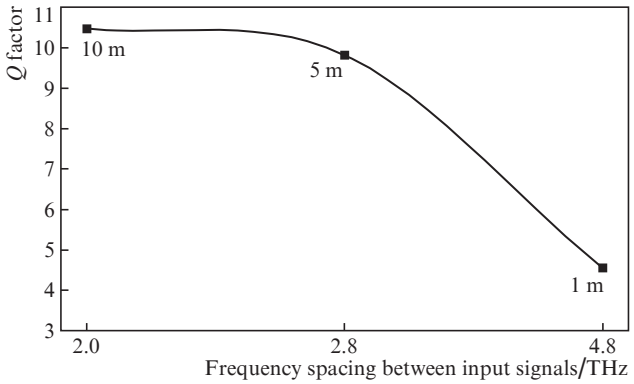

Figure 12. Quality factor of the wavelength converted signal and input channel spacing (at 3 dB falling from maximum conversion efficiency) vs. fibre length.

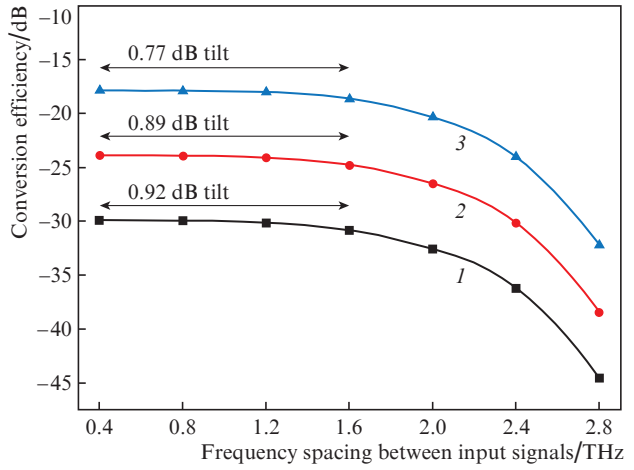

Figure 13. Conversion efficiency (CSRZ-DQPSK signal) vs. channel frequency spacing for the different input powers of (*1*) 0, (*2*) 2, and (*3*) 4 dBm.

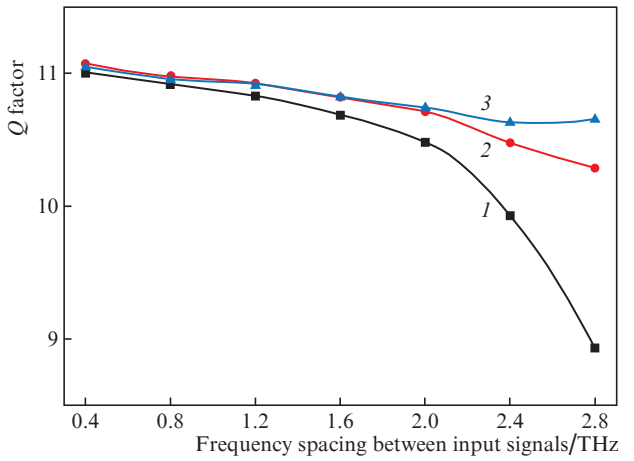

Figure 14. Quality factor (CSRZ-DQPSK signal) vs. channel frequency spacing for the different input powers of (*1*) 0, (*2*) 2, and (*3*) 4 dBm.

signal on the input signal frequency spacing for the different fibre lengths. As depicted in Fig. 11, the conversion efficiency bandwidth is improved to 144 nm for the 1 m long fibre where the input channel frequency spacing is 4.8 THz and the input signal power is 1 mW. Figure 12 shows that the observed Q factor for the wavelength converted signal is 4.54. By increasing the input signal power, the conversion efficiency and Q factor can be improved to significant levels. Figures 13 and 14 show the conversion efficiency and Q factor improvement for the different input powers at a fibre length of 10 m.

As the input signal power increases, the conversion efficiency also increases as shown in Fig. 13. This input power variation also facilitates further flattening of conversion efficiency to a noteworthy level. For an input power of 4 dBm, a flattened conversion efficiency of –17.86 dB is obtained with a 0.77 dB deviation up to 1.6 THz. The Q factor of the wavelength converted signal also gets improved and the dispersion curve is more flattened as depicted in Fig. 14. For the input power of 4 dBm the Q factor of the CSRZ-DQPSK signal is improved from 8.93 to 10.65 even for 2.8 THz frequency spacing between the input signals.

4. Conclusions

We have demonstrated 80 Gb s^{-1} two channel wavelength conversion using the FWM technique in our newly designed HN-UFF without additional pump signals. The conversion efficiency of the wavelength converted signals is –29.9 dB with a variation of 0.92 dB up to 1.6 THz frequency spacing between the input signals. The obtained Q factor is also very flat over this frequency range of 2 THz due to the flattened dispersion and nonlinear characteristics of HN-UFF. When compared with RZ-DQPSK, CSRZ-DQPSK modulation gives higher conversion efficiency, thus improving significantly the system performance. Also, the Q factor is improved to 11.01 for CSRZ-DQPSK compared to RZ-DQPSK which has the value of 9.83. Beyond the 1.6 THz frequency spacing, the uniformity of the conversion efficiency gets affected, but the quality of the signal remains very good when CSRZ-DQPSK modulation is used. The impact of the input power on conversion efficiency is also observed up to 4 dBm. The input power variation improves the conversion efficiency and provides greater flattening. For the input power of 4 dBm, the observed flattened conversion efficiency for the fibre length of 10 m is –17.86 dB with a variation of 0.77 dB. The designed system, with the CSRZ-DQPSK signal and our newly designed HN-UFF, delivers a power penalty of 0.76 dB up to the 2 THz of input channel spacing.

We have also studied the impact of fibre length variation on the conversion efficiency bandwidth. For a 10 m length of fibre, the obtained conversion efficiency is –29.9 dB with a limited conversion efficiency bandwidth of 48.6 nm. But for a 1 m long fibre, the wideband wavelength conversion bandwidth of 144 nm is reached with a Q factor of 4.6 and the measured maximum conversion efficiency is –49.85 dB. Further improvement on this conversion efficiency and Q factor is possible by increasing the input. This flattened conversion efficiency and Q factor reduce the frequency dependent limitation in FWM-based wavelength conversion for its transparency and give a wide range of tunable option in frequency spacing chosen for wavelength conversion in the future optical networks.

Acknowledgements. The authors thankfully acknowledge the Department of Science and Technology (DST), New Delhi for their Fund for the Improvement of S&T Infrastructure in

Universities and Higher Educational Institutions – (FIST) grant through the order No. SR/FST/College-061/2011(C) to procure the OptiWave simulation package.

References

1. Kibria R., Austin M.W. *IEEE Photon. J.*, **2**, 200 (2015), DOI:10.3390/photonics2010200.
2. Wang D., Cheng T.-H., Yeo Y.-K., Xu Z., Wang Y., Xiao G., Liu J. *IEEE J. Lightwave Technol.*, **28** (24), 3497 (2010).
3. Weber H.-G., Nakazawa M. *Ultrahigh-Speed Optical Transmission Technology* (Berlin: Springer, 2007) pp 141–165.
4. Anthur A.P., Venkitesh D. *Opt. Commun.*, **338**, 149 (2015).
5. Wu X., Huang H., Wang J., Wang X., Yilmaz O.F., Nuccio S.R., Willner A.E. *Proc. Conf. Lasers and Electro-Optics (CLEO) and Quantum Electronics and Laser Science (QELS)*, **1–2**, 16 (2010).
6. Anthur A.P., Watts R.T., O'Duill S., Zhou R., Venkitesh D., Barry L.P. *IEEE J. Quantum Electron*, **51**, 1 (2015).
7. Liang Wang, Chester Shu. *Opt. Commun.*, **338**, 384 (2015).
8. María R. Fernández-Ruiz, Lei Lei, Martin Rochette, José Azaña. *Opt. Express*, **23** (17), 22847 (2015), DOI:10.1364/OE.23.022847.
9. Marhic M.E., Andrekson P.A., Petropoulos P., Radic S., Peucheret C. , Jazayerifar M. *Laser Photon. Rev.*, **9** (1), 50 (2014); DOI:10.1002/lpor.201400087.
10. Rancaño V.J.F., Jain S., May-Smith T.C., Hugues-Salas E., Shuangyi Yan, Zervas G., Simeonidou D., Petropoulos P., Richardson D.J. *IEEE Photon. Technol. Lett.*, **27** (8), 828 (2015).
11. Anlin Yi, Lianshan Yan, Bin Luo, Wei Pan, Lin Jiang, Zhiyu Chen, Yan Pan. *IEEE Photon. J.*, **7** (1), 1 (2015), DOI:10.1109/JPHOT.2015.2402155.
12. Zhu P., Li J., Wu Z., XinChen, Xu Y., Lin B., Chen Z., He Y. *Opt. Commun.*, **347**, 25 (2015).
13. Chagnon M., Spasojevic M., Adams R., Li J., Plant D.V., Chen L.R. *IEEE Photon. Technol. Lett.*, **27** (8), 860 (2015).
14. Chen M., Yang J., Zhang N., Youa S. *Opt. Eng.*, **54** (5), 056109 (2015).
15. Zhou G.T., Xu K., Wu J., Yan C., Su Y., Lin J.T. *IEEE Photon. Technol. Lett.*, **18** (22), 2389 (2006).
16. Selvendran S., Sivanantharaja A., Kalaiselvi K., Esakkimuthu K. *Opt. Quantum Electron.*, **45** (2), 135 (2013).
17. Shunsuke O., in *Optical Fiber New Developments* (Winchester: InTech, 2009) pp 495–514, DOI:105772/7558.
18. Fatih Y. *Fiber-Optic Parametric Amplifiers: Their Advantages and Limitations. Master Thesis* (New York: University of Rochester, 2006).
19. Inoue K. *IEEE J. Lightwave Technol.*, **10** (11), 1553 (1992).
20. Bass M., van Stryland E.W. *Fiber Optics Handbook: Fiber, Devices and Systems for Optical Communications* (New York: McGraw-Hill, 2002).
21. Hirano M., Nakanishi T., Okuno T., Onishi M. *IEEE J. Sel. Top. Quantum Electron.*, **15** (1), 103 (2009).
22. Selvendran S., Sivanantharaja A. *J. Nonlinear Opt. Phys. & Mater.*, **22** (3), 1350034 (2013), DOI:10.1142/S0218863513500343.
23. Selvendran S., Sivanantharaja A., Arivazhagan S., Kannan M. *Quantum Electron.*, **46** (9), 829 (2016) [*Kvantovaya Elektron.*, **46** (9), 829 (2016)].